Enhanced long-term potentiation in mature rats in a model of epileptic spasms with betamethasone-priming and postnatal *N*-methyl-D-aspartate administration

*†Megumi Tsuji, *Yukari Takahashi, *‡Ayako M. Watabe, and *Fusao Kato

Dr. Megumi Tsuji is a pediatric neurologist at Kanagawa Children's Medical Center, Yokohama, Japan.

SUMMARY

Objective: Patients with epileptic spasms are at high risk for learning and memory impairment later in life. We examined whether synaptic plasticity is affected in the adult hippocampus, a structure responsible for learning and memory, using an animal model of epileptic spasms of unknown cause.

Methods: We produced a rat model of *N*-methyl-D-aspartate (NMDA)–induced spasms combined with prenatal betamethasone administration. In 6- to 11-week-old rats, we evaluated the long-term potentiation (LTP) and general properties of synaptic transmission in pyramidal neurons in the CA1 area of the hippocampus in brain slices.

Results: The magnitude of LTP by theta burst stimulation was significantly larger in adult rats with a history of infantile NMDA injections than in control rats and rats that received additional adrenocorticotropic hormone (ACTH) treatment. The frequency of spontaneous excitatory transmission, but not inhibitory transmission, was smaller in adult rats with a history of infantile NMDA injections.

Significance: This study is the first to provide a basis for the alteration of synaptic plasticity and transmission in a model of epileptic spasms of unknown cause. Postnatal NMDA treatment causing epileptic spasms–like aberrant episodes in the early stage of life in rats has a latent influence on various forms of synaptic plasticity in the hippocampus. Our results provide a novel insight into cognitive impairment that appears later in life in patients with a history of epileptic spasms.

KEY WORDS: Epileptic spasms, Animal model, Prenatal stress, Hippocampus, Synaptic plasticity, Long-term potentiation.

West syndrome is a specific type of catastrophic epileptic syndrome occurring only in infancy and early childhood, which is characterized by (1) a specific electroencephalog- raphy (EEG) abnormality termed hypsarrhythmia, (2) epileptic spasms with truncal flexion, and (3) psychomotor deterioration.[1] Of these, the epileptic spasms (formerly ter- med infantile spasms) is the most apparent age-dependent phenotype that has serious neurologic consequences later in life regardless of the disappearance of early symptoms.[2] In particular, impaired learning and memory function appear in a large majority of adult patients with a history of epilep- tic spasms.[3–6] Such remote and latent neurologic outcomes do not seem to be linked directly with how the epileptic epi- sodes were controlled, such as with drugs, during infancy.[2] Therefore, it is important to address the question of how these symptoms in infancy exert remote and latent influ- ences on cognitive brain function later in life.[7]

Apart from the West syndrome subclasses with identifi- able "genetic" or "structural-metabolic" (formerly termed

KEY POINTS

- We evaluated synaptic transmission in adult rats in a model of epileptic spasms created by prenatal steroid priming and postnatal NMDA injections
- ACTH significantly altered the frequency distribution of motion arrest observed following NMDA injection
- The magnitude of LTP was significantly larger in adult hippocampal slices from rats with a history of NMDA-induced epileptic spasms than in those in control and ACTH treatment groups
- NMDA-dependent epileptic spasms have a latent influence on various forms of synaptic plasticity in the hippocampus

"symptomatic") causes, which have several genetically modified mouse models with similar epileptic and neurologic abnormalities,[8–12] epileptic spasms with unknown cause (formerly termed "cryptogenic") have only a few proposed animal models. Of these, we used an animal model without any genetic manipulation developed recently by Velíšek et al.,[13–15] as it allows analysis of the remote and latent influences of epileptic spasms on the higher functions in adults after maturation. This has an advantage over the genetics models, in which the phenotype in adults could result not only from the spasms in the infantile period but also from the genetic deficiency.

The model uses *N*-methyl-D-aspartate (NMDA) as a trigger to elicit a series of truncal flexion spasms, which are similar to those observed in human patients and specific spasm-associated EEG abnormalities in the early stages of life. It is also the sole model for epileptic spasms of unknown cause that is responsive to adrenocorticotropic hormone (ACTH), a treatment recommended globally for epileptic spasms of unknown cause in humans.[16] It is notable that this model does not show spontaneous spasms after the early period and that the rats are able to mature to adulthood. Taking advantage of this, we analyzed synaptic function in the hippocampus—a structure responsible for learning and memory—of adult rats that had shown typical spasms only in the early period. We examined whether synaptic plasticity is affected in this model as in other types of epilepsy such as thermal seizures[17] and hypoxia-induced seizures.[18] A part of this study was reported previously at the Annual Meeting of the Society for Neuroscience in 2013.[19]

MATERIALS AND METHODS

The manipulation of animals was approved by the Institutional Animal Care and Use Committee of Jikei University and conformed to the Guidelines for the Proper Conduct of

Animal Experiments of the Science Council of Japan (2006).

Epileptic spasms model

The animal model for epileptic spasms was produced according to a previous report.[15] Briefly, pregnant Sprague-Dawley rats were treated with betamethasone twice on gestational day 15 (G15; 0.4 mg/kg, i.p., at 09:00 and 18:00) and their offspring were raised with the dam with free access to food and water with a regular light/dark cycle (light, 07:00–19:00). The male offspring were divided randomly into "control," "NMDA," and "NMDA/ACTH" groups, with distinct pharmacologic treatments afterwards (Table 1). The NMDA and NMDA/ACTH groups received i.p. injections of NMDA solution (1.5 mg/mL dissolved in saline) on postnatal day (P) 12, P13, and P15 at 09:00–10:00. The doses were 7.5, 12, and 15 mg/kg on P12, P13, and P15, respectively. The control group received physiologic saline of the same volume. The NMDA/ACTH group additionally received ACTH (0.3 mg/kg, s.c.; 0.1 mg/ml: twice at 14:00 and 21:00 on P12 and three times at 09:00, 14:00, and 21:00 on P13 and P14).[15] The control and NMDA groups received the same volume of saline instead of ACTH. After weaning at P21, the rats were raised with normal chow and water with free access on the same light/dark cycle as above until postnatal weeks 6–11. The age at which the postmaturational analyses were done is summarized in Table 2.

Spasms analysis

Each rat at P12 or P15 was put in an acrylic glass transparent cylinder with a diameter of 12 cm immediately after the NMDA or saline injection. Spasm analysis was made twice for every rat on P12 (to evaluate first NMDA challenge) and on P15 (to evaluate the effect of 3-day administration of ACTH). Spontaneous movement was video-captured on a four-cylinder-in-a-frame basis using a high-definition camera and webcam capture software (c525; Logitech, Tokyo, Japan) at 15 frames/s for 2 h. Movie files were converted to QuickTime movie format with video-editing software (Video Mastering Works 5; Pegasys, Tokyo, Japan) and read into Igor Pro 6 (WaveMetrics, OR, U.S.A.). After selecting a rectangular region of interest for each rat (e.g., insets in Fig. 1A, B), the square mean of the frame-to-frame difference for the region of interest was calculated, and the moving average of this difference over 15 frames (i.e., 1 s) was calculated for the whole span of the captured video. These values were plotted as a function of frame number (i.e., time) and defined as "movement function" (Fig. 1A,B), which was used for detecting specific activity patterns. The behavior of the animal was continuously monitored from above the chamber, and we classified the behavioral status according to the previously described criteria.[13]

Table 1. Experimental treatments in each group and protocols at each developmental stage

Age	Prenatal (G15)		P12–P15 (infancy)		6–11 Weeks (adulthood)
Group name	Betamethasone injections	NMDA (i.p.) injections	Movement analysis	ACTH (s.c.) injections	Electrophysiologic analyses of slices
NMDA	0.4 mg/kg (i.p.) ×2	3 times at P12 (7.5 mg/kg), P13 (12 mg/kg) P15 (15 mg/kg) (same cohort)	2 times at P12 + P15 (same cohort)	Saline ×8	Field EPSP or whole-cell recording (different cohorts)
NMDA/ACTH	As above	As above	As above	8 times at P12 × 2 (14:00, 21:00) P13 × 3 (9:00, 14:00, 21:00) P14 × 3 (9:00, 14:00, 21:00) 0.3 mg/kg for each (same cohort)	As above
Control	As above	Saline ×3	As above	Saline ×8	As above

Table 2. Summary of the age of rats (postnatal day) used for each test

Groups	Field EPSP recording	NMDA/AMPA ratio	Spontaneous synaptic transmission analyses
Control	50.3 (42–71) [16]	57.9 (42–78) [10]	49.4 (42–61) [15]
NMDA	51.5 (43–75) [13]	62.5 (46–78) [12]	53.4 (42–62) [18]
NMDA/ACTH	52.2 (43–68) [16]	62.8 (47–77) [11]	55.5 (47–61) [16]
ANOVA p-Value	0.884	0.660	0.076

Average, range (in the parenthesis) and the number of slices (in brackets). There was no significant difference between groups in any tests.

Field potential recordings and long-term potentiation (LTP) induction

Hippocampal slices were prepared as described previously.[20] Briefly, the animals were anesthetized deeply with isoflurane, and the brain was removed rapidly and placed in ice-cold cutting solution consisting of (in mM) 125 NaCl, 3.0 KCl, 25 $NaHCO_3$, 1.25 NaH_2PO_4, 5.0 $MgCl_2$, 0.1 $CaCl_2$, 12.5 glucose, and 0.4 L-ascorbic acid (gassed with 95% O_2/ 5% CO_2). The hippocampus was extracted quickly, and 400-µm thick transverse slices were prepared using a vibrating blade slicer (Pro 7; Dosaka, Kyoto, Japan) and transferred to an interface-type recording chamber (Fine Science Tools, Foster City, CA, U.S.A.), where they were perfused continuously (2 ml/min) with artificial cerebrospinal fluid (aCSF) containing (in mM) 124 NaCl, 4.4 KCl, 25 $NaHCO_3$, 2.0 $CaCl_2$, 1.2 $MgSO_4$, 1.0 NaH_2PO_4, and 10.0 D-glucose saturated with 95% O_2/5% CO_2. The slices were maintained in the chamber at 30°C for >30 min before recording.

A glass microelectrode made from a borosilicate pipette (G150F-3; Warner Instruments) was filled with aCSF and placed in the stratum radiatum of the CA1 region to record field excitatory postsynaptic potentials (fEPSPs). The field potentials were amplified with AxoPatch 1D (Axon Instruments, Union City, CA, U.S.A.) and digitized with DigiData 1322A (Axon Instruments) at 10 kHz and 16-bit resolution using pClamp software (Axon Instruments). fEPSPs were evoked with a parallel bipolar electrode (interpolar distance,

50 µm; Unique Medical, Tokyo, Japan) connected to a constant voltage isolator driven by Master-8 (A.M.P.I., Jerusalem, Israel). The stimulation electrode was placed in the middle of the stratum radiatum. The test stimulus (100 µs duration) was delivered every 10 s with a stimulation intensity set to elicit half of the maximum response. After obtaining a stable baseline for 20 min, LTP was induced by applying theta burst stimulation (TBS; five trains of four pulses at 100 Hz with an intertrain interval of 200 msec, delivered twice at an interval of 10 s). The slopes of six consecutive fEPSPs (1 min recording) were averaged and normalized to the mean value over the 20-min baseline period. In a few cases in which the fEPSP slope during this 20 min baseline period changed by >10% or if the fEPSP slope became unexpectedly smaller than the pre-TBS value during post-TBS recording, the data for these cases were discarded and excluded from the statistical analyses. Paired-pulse stimulations at an interstimulus interval of 100 msec were delivered before this baseline period to estimate the paired-pulse ratio (PPR).

Whole-cell recording of postsynaptic currents

Coronal slices of the dorsal hippocampus (400-µm thick) were prepared according to the method described previously.[21] The following cutting solution was used (in mM): 92 N-methyl-D-glucamine, 2.5 KCl, 30 $NaHCO_3$, 1.25 NaH_2PO_4, 0.5 $MgSO_4$, 0.5 $CaCl_2$, 25 glucose, 5 L-ascorbic
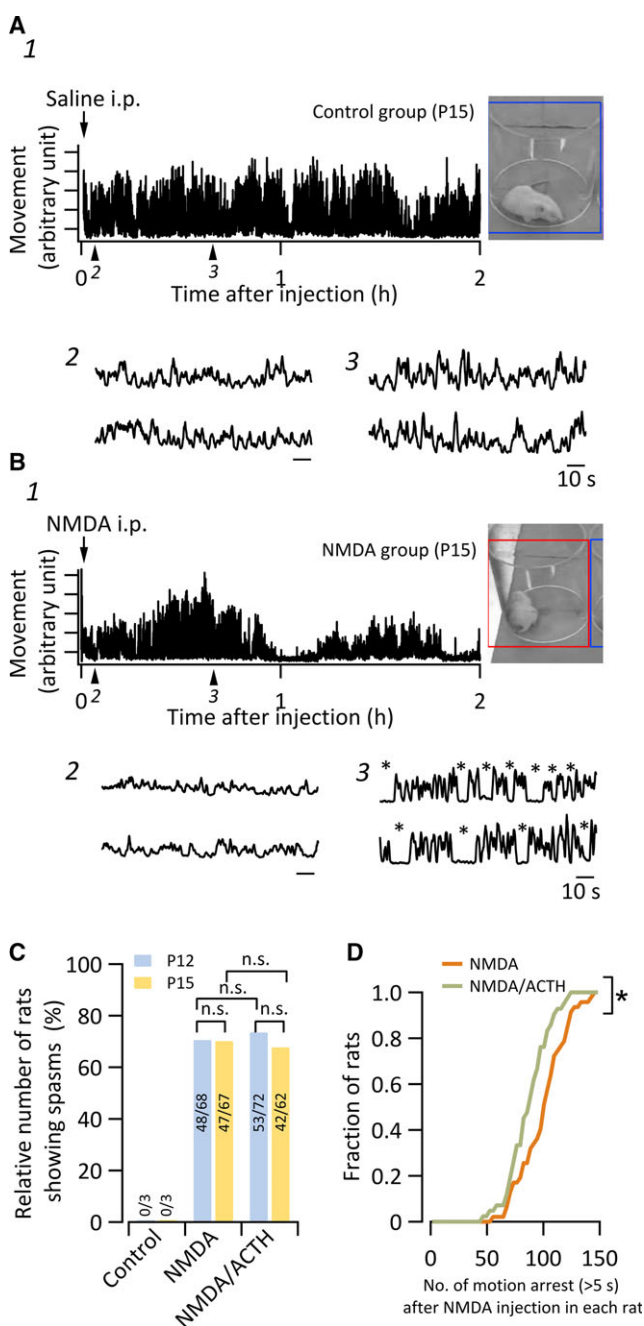
Figure 1.
Effects of NMDA injection on spontaneous movements in betamethasone-primed infant rats. (**A**, **B**) Time course of spontaneous movements after intraperitoneal injections of saline (**A**, a rat from control group) or 15 mg/kg NMDA (**B**, a rat from NMDA group) at time 0. (A2) and (B2), extended versions of baseline recordings before injections indicated with numbered arrowheads 2 in (A1) and (B1), respectively. (A3) and (B3), time-extended traces of the recordings at 40 min after injections indicated with numbered arrowheads 3 in (A1) and (B1). Note that NMDA injection, but not that of saline, gave rise to a specific pattern of repeated appearance of motion arrest (asterisks in B3). Inset pictures on the right show representative samples of the digital images, based on which frame-to-frame pixel differences were evaluated to obtain the movement functions in (A1) and (B1). See text for details. The time scales for (A2), (A3), (B2), and (B3) are the same. (**C**) Relative number of rats showing any spasms within 2 h following NMDA injection normalized by the total number of rats examined. Pale blue bars, values for the post-NMDA measurement made at P12; yellow bars, those at P15. Rats belonging to the control group that received saline instead of NMDA did not show any spasms ("Control"). (**D**) Cumulative histogram indicating the fraction of rats showing respective number of motion arrest (>5 s) during 2-h observation after NMDA injection. Ordinate, fraction of rats; Abscissa, number of motion arrests longer than 5 s in each rat. Based on the measurements at P15. Orange curve, NMDA group (n = 47 rats); olive green curve, NMDA/ACTH group (n = 42 rats). *p < 0.05, Kolmogorov-Smirnov test.
Epilepsia © ILAE

acid, 2 thiourea, 5 pyruvate, 20 4-(2-Hydroxyethyl)piperazine-1-ethanesulfonic acid (HEPES), and 12 N-acetyl-L-cysteine (gassed with 95% O_2/5% CO_2). The same aCSF as above was used for the recordings. The CA1 region was disconnected from the CA3 region with a surgical knife. Whole-cell current and membrane potential were recorded from visually identified pyramidal neurons in CA1 with infrared differential interference contrast (IR-DIC) optics (BX-51WI; Olympus, Tokyo, Japan). The patch-clamp electrodes were made of borosilicate glass pipettes (1B120F-4; World Precision Instruments). The internal solution was composed of either (1) (in mM) 135 K-gluco-

nate, 10 HEPES, 1 ethylene glycol-bis(2-aminoethylether)-N,N,N',N'-tetraacetic acid (EGTA), 0.1 $CaCl_2$, 2 $MgCl_2$, 2 ATP, and 0.3 guanosine 5'-triphosphate (GTP), or (2) 136 CsCl, 10 HEPES, 5 EGTA, 12 Na_2-phosphocreatine, 1 $CaCl_2$, and 2 ATP with 5 QX-314. Solution (1) was used for simultaneous recording of spontaneous excitatory postsynaptic currents (sEPSCs) and inhibitory postsynaptic currents (sIPSCs); at a holding potential of -60 mV, sEPSCs and sIPSCs were recorded as inward and outward currents, respectively.[21] Solution (2) was used for recording the NMDA receptor- and alpha-amino-3-hydroxy-5-methyl-4-isoxazolepropionic acid (AMPA) receptor–mediated EPSCs to calculate the NMDA/AMPA ratio (the amplitude of NMDA receptor–mediated EPSCs relative to that of AMPA receptor–mediated EPSCs). This recording was made in the presence of 100 μM of picrotoxin to block γ-aminobutyric acid (GABA)$_A$ receptor–mediated components. The NMDA current was recorded at +40 mV in the presence of 10 μM 6-cyano-7-nitroquinoxaline-2,3-dione disodium salt (CNQX). The tip resistance of the electrode was 4–8 MΩ. EPSCs were evoked by bipolar stimulation of Schaffer collaterals (100 μs, 0.1 Hz) at a constant current intensity that was fixed so that EPSC amplitude became approximately 200 pA. Paired-pulse stimulations at an interstimulus interval of 100 msec were delivered before recordings of spontaneous activities to esti-

mate PPR of evoked EPSC amplitude. A small and short hyperpolarizing command (-10 mV; 10–20 msec) was applied at 25–100 msec before each stimulus to monitor continuously the changes in series resistance, membrane capacitance, and input resistance. When series resistance was changed by >25%, the recording was discarded. Compensation for membrane capacitance, but not series resistance, was performed. Membrane potentials are shown without compensation for liquid junction potential. Membrane current or membrane potential was recorded using an Axopatch 200B amplifier (Axon Instruments), low-pass filtered at 2 kHz, and sampled at 10 kHz with 16-bit resolution using a PowerLab interface with LabChart software (ADInstruments, BioResearch, Nagoya, Japan).

Drugs

Rat ACTH (1–39) was obtained from GenScript (Piscataway, NJ, U.S.A.). Betamethasone, NMDA, CNQX, and picrotoxin were purchased from Sigma-Aldrich (St. Louis, MO, U.S.A.). Other chemicals were purchased from Sigma-Aldrich and Nacalai-tesque (Kyoto, Japan).

Data analysis and statistics

The fEPSP data were analyzed using pClamp (Axon Instruments) and Microsoft Excel according to standard methods. The EPSC and IPSC data were analyzed using IgorPro 6 (WaveMetrics) with a program written by F.K. The EPSCs and IPSCs were detected by template-based fitting, and all detected events were confirmed visually. The frequencies of sEPSCs and sIPSCs were evaluated based on data from a stable 5-min recording period. Statistical comparisons were made using SPSS (IBM, Japan). For comparison of relative number of rats showing any spasms, Fisher's exact probability test or Pearson's chi-square test was used. The distribution of frequency of motion arrests observed in each rat and the distribution of mean sEPSC and sIPSC frequency were evaluated with the Kolmogorov-Smirnov test, and the results are shown with cumulative histograms. The degree of LTP, the frequency and amplitude of PSCs, and the AMPA/NMDA ratio between the three groups were evaluated using one-way analysis of variance (ANOVA) followed by Tukey's post hoc test. The effects of ACTH treatment and spasms occurrence on fEPSP were compared with two-way ANOVA. Student's *t*-test was used for comparison between two groups with or without spasms. Detection of significant outlier value was performed by Grubbs' test (also called the extreme studentized deviate test) using the GraphPad Prism website. A probability value <0.05 was considered statistically significant.

RESULTS

NMDA-triggered spasms in a model of epileptic spasms

Figure 1A,B show representative results of the movement of rats in the control and NMDA groups, respectively.

After injection of NMDA, the rats showed sudden motion arrest (marked with asterisk in Fig. 1B3) associated with specific truncal flexion spasms that lasted for 5–30 s and occurred repeatedly. This spasm phase appeared in-between phases of hyperactive aimless walking with tail twisting (Fig. 1B2,3). Such motion arrest did not appear in control rats (Fig. 1A1–3).

We failed to detect a significant difference in the relative number of rats that showed any spasms between the NMDA and NMDA/ACTH groups at P12 and P15 (Fig. 1C) and also between P12 and P15 (Pearson's chi-square test; Fig. 1C). However, there were significant differences between the groups in the frequency of observed spasm-associated motion arrest. Figure 1D indicates the cumulative histogram with the fraction of rats (ordinate) showing the respective number of motion arrest longer than 5 s observed within 2 h after NMDA injection (shown in abscissa). This analysis shows the distribution of how often each rat showed spasm-associated motion arrests. Despite no significant difference in the number of rats showing spasms of any duration (Fig. 1C), the motion arrests longer than 5 s were less frequently observed in rats in the NMDA/ACTH group than in the NMDA group at P15 ($p = 0.007$; n = 47 and 42, respectively; Kolmogorov-Smirnov test; Fig. 1D), but not at P12, suggesting that the 3-day application of ACTH significantly reduced the severity of the spasm expression. The mortality rate at P12 (before ACTH series) was 7 (5%) of 140 rats, that at P13–P15 for NMDA/ACTH group was 5 (8.2%) of 61 rats, and that for NMDA group was 4 (6.3%) of 63 rats. There was no significant difference between these ratios ($p = 0.52$–0.74; Fisher's exact probability test). Such typical occurrences of motion arrest and flexion spasms after NMDA injection are highly similar to the behavioral features of the model described by Velíšek et al.[13]

TBS induces enhanced LTP in the NMDA group in the CA1 region of the hippocampus

We assessed the LTP of synaptic transmission in the hippocampus CA1 region in adult rats (6–11 weeks postnatal) in the control, NMDA, and NMDA/ACTH groups. TBS induced robust LTP in all three groups (n = 16 slices from 8 rats from 4 dams, 13 slices from 10 rats from 5 dams, and 16 slices from 9 rats from 5 dams) for the control, NMDA, and NMDA/ACTH groups, respectively), but its magnitude was significantly larger in the NMDA group than in the control and NMDA/ACTH groups (Fig. 2A1). The mean relative fEPSP slope at 36–45 min after TBS (fEPSP slope$_{36–45}$) was significantly larger in slices from the NMDA group than in those from the control and NMDA/ACTH groups ($F_{2,42} = 5.11$; ANOVA with Tukey's post hoc test; $p = 0.010$; Fig. 2A2). Two-way ANOVA analysis of fEPSP slope$_{36–45}$ in the rats given NMDA injections revealed a significant effect of ACTH treatment ($F = 5.692$; $p = 0.025$; Fig. 2A2) without a significant effect of spasm occurrence
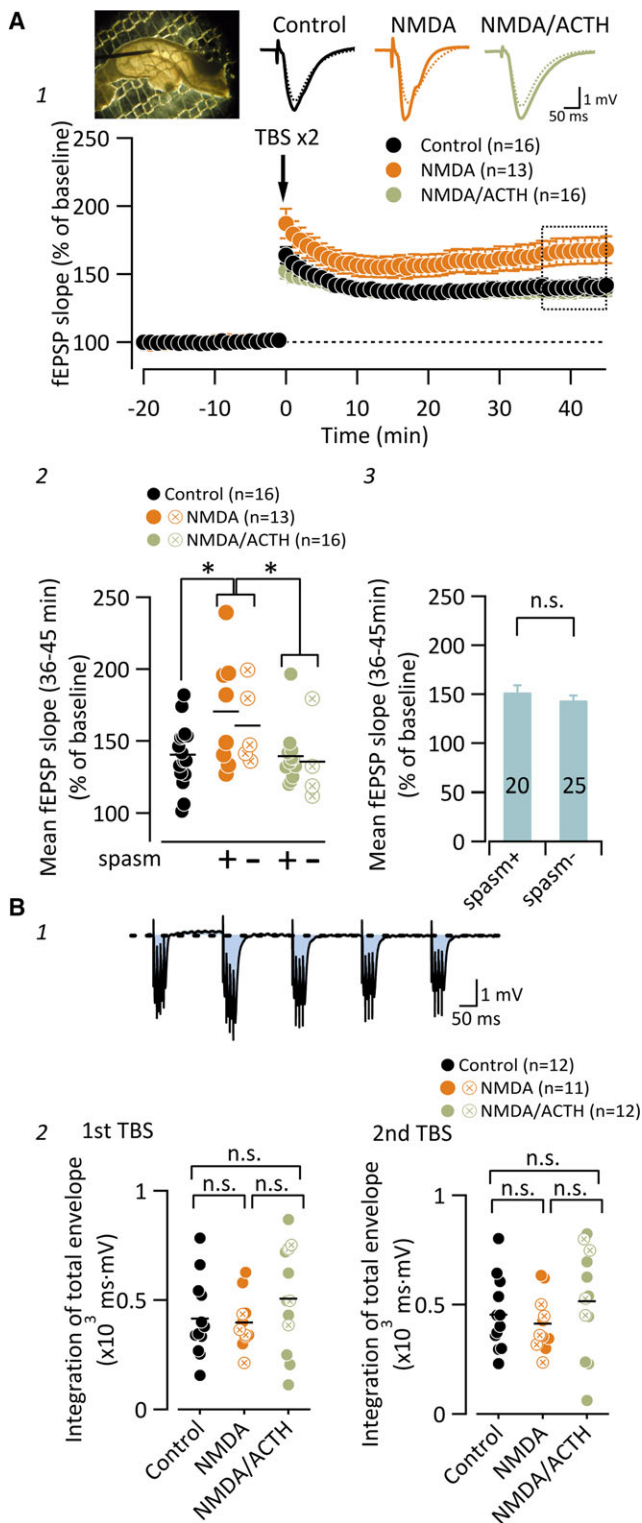
Figure 2.
Analysis of synaptic plasticity in the adult hippocampus from rats with infantile NMDA injections. (A1) Summary of the time course of fEPSP slope in hippocampal slices prepared from rats from control (black circles), NMDA (orange circles), and NMDA/ACTH (olive green circles) groups. The inset above shows a picture of a representative hippocampal slice being used for field recording (left) and the representative fEPSP traces (averages of six responses) recorded in CA1 regions from rats belonging to control (black traces), NMDA (orange traces), and NMDA/ACTH (olive green traces) groups. Thin dashed curves, at 1 min before TBS; thick solid curves, at 45 min post-TBS. Error bars represent standard error of the mean (SEM). (A2) Summary of fEPSP slope measured at 36–45 min post-TBS in individual slices from control (black filled circles), NMDA (orange circles), and NMDA/ACTH (olive green circles) groups. The circles with "X" indicate the values for slices from rats showing no detectable spasms within 2 h after NMDA injection at P15. No rat in control groups showed spasms. Black horizontal bars indicate the mean for each group. *$p < 0.05$, one-way ANOVA, with post hoc Tukey test. The two-way ANOVA (effects of spasm and ACTH) indicated the significant effect ($p = 0.025$) of ACTH (see text for details). (A3) Mean fEPSP slope$_{36–45}$ in the rats with and without post-NMDA spasms (spasm+ and spasm−, respectively). Data from NMDA and NMDA/ACTH groups are pooled and re-classified according to the occurrence of spasms. n.s., not significantly different; Student's t-test. (B1) A representative trace of the field recording during TBS. (B2) Summary of responses during TBS as evaluated by integrating the envelope (area of the pale blue–shaded zone in [B1]). Control (black circles), NMDA (orange circles), and NMDA/ACTH (olive green circles) groups. The circles with "X" indicate the values for slices from rats showing no detectable spasms within 2 h after NMDA injection at P15. The horizontal bars indicate the means for each group. n.s., not significantly different (one-way ANOVA).
Epilepsia © ILAE

ined whether these groups contained "outlier" values using Grubbs' test. The largest value in the NMDA group was not judged to be a significant outlier ($p > 0.05$) but the largest value in NMDA/ACTH group was judged to be a significant outlier ($p < 0.05$). However, the omission of the latter value from the statistics did not affect the statistical conclusions described and was retained in the graph.

To examine whether the spasms experience itself affects the LTP magnitude at the postmaturation stage, we compared fEPSP slope$_{36–45}$ between all slices from rats with and without detectable spasms at P15 regardless of the pharmacologic intervention (Fig. 2A3). There was no significant difference between these values from rats with and without spasms, indicating that spasms experience itself is not the principal factor in determining the LTP magnitude. Inclusion or omission of the outlier value described above from the NMDA/ACTH group did not affect this statistical conclusion.

There was no significant difference in the depolarization envelope during TBS evaluated from the area of the down-

at P15 ($F = 0.331$; $p = 0.57$; circles marked with an "X" in Fig. 2A2) and an interaction between spasm occurrence and ACTH treatment ($F = 0.065$; $p = 0.80$; Fig. 2A2). Because the distribution of fEPSP slope$_{36–45}$ was wide especially in NMDA and NMDA/ACTH groups (Fig. 2A2), we exam-

ward traces (pale blue–shaded areas in Fig. 2B1), between three groups (Fig. 2B2; 1st TBS: $F_{2,32} = 1.123$, p = 0.338; 2nd TBS: $F_{2,32} = 0.877$, p = 0.426, ANOVA). In line with this, we failed to observe significant difference in the paired-pulse ratio (PPR) between groups (1.47 ± 0.02, 1.48 ± 0.01, and 1.49 ± 0.02 for control, NMDA, and NMDA/ACTH groups, respectively; p = 0.79–0.90; ANOVA, $F_{2,64} = 0.156$). Of interest, when tetanus stimulation (100 Hz, 1 s, twice) was used to elicit LTP instead of TBS, we failed to detect a significant difference in LTP magnitude between the groups (traces not shown); the fEPSP slope at 36–45 min after tetanus was $164.0 \pm 10.5\%$, $161.2 \pm 18.7\%$, and $168.5 \pm 13.6\%$ in the control, NMDA, and NMDA/ACTH groups, respectively (n = 4, 5, and 6, respectively; $F_{2,12} = 0.45$; ANOVA, Tukey's post hoc test; p = 0.65).

Synaptic transmissions in pyramidal neurons in the CA1

sEPSCs and sIPSCs were recorded simultaneously from CA1 pyramidal neurons in slices prepared from adult rats with a history of infantile NMDA injection (Fig. 3A). Figure 3B shows the distribution of the mean frequency of sEPSCs (left) and sIPSCs (right) in each neuron recorded in slices prepared from the three groups. The cumulative probability plots for the mean sEPSC (left) and sIPSC (right) frequency of the neurons indicate that the distribution of mean sEPSC frequency of the neurons from the NMDA group was significantly different from that of the control group (p = 0.048, Kolmogorov–Smirnov test; Fig. 3B). In addition, there was a significant difference in sEPSC frequency between neurons from the NMDA/ACTH and control groups ($F_{2,46} = 3.269$; ANOVA; p = 0.047, Tukey's post hoc test; n = 15, 18, and 16 for the control, NMDA, and NMDA/ACTH groups, respectively, Fig. 3C left). In contrast, there was no difference in sIPSC frequency between any of the three groups ($F_{2,46} = 0.59$; p = 0.81, ANOVA; Fig. 3C right). There was no significant difference in the amplitude of sEPSCs and sIPSCs between the three groups ($F_{2,46} = 2.097$ and $F_{2,46} = 1.204$; p = 0.13 and p = 0.31 for sEPSC and sIPSC amplitude, respectively, ANOVA; Fig. 3D). We failed to observe a significant difference in PPR between groups (1.56 ± 0.06, 1.53 ± 0.06 and 1.50 ± 0.05 for control, NMDA and NMDA/ACTH groups, respectively; p = 0.40–0.82; ANOVA, $F_{2,64} = 0.232$). For the rats from which these postsynaptic currents were recorded, 0 of 15, 18 of 18, and 6 of 16 rats showed any spasms for control, NMDA, and NMDA/ACTH groups, respectively. There was no significant difference in the frequency as well as in the amplitude of sEPSCs and sIPSCs between rats with and without any spasms after NMDA injections (Fig. 3C,D, second and fourth graphs from the left). These results suggest that in the hippocampus of the NMDA group, the fraction of neurons receiving spontaneous excitatory inputs at a higher frequency was reduced.

To evaluate the contribution of NMDA receptor–mediated components in the postsynaptic responses, the NMDA/ AMPA ratio were assessed (Fig. 4). There was no significant difference in the NMDA/AMPA ratio between any of the groups ($F_{2,30} = 0.084$, p = 0.92, ANOVA, Tukey's post hoc test, n = 10, 12, and 11 for the control, NMDA, and NMDA/ACTH groups, respectively, Fig. 4B). Between the three groups, there was no significant difference in the stimulation intensity required to evoke EPSCs with an amplitude of approximately 200 pA ($F_{2,30} = 0.225$, p = 0.80; ANOVA, Tukey's post hoc test, Fig. 4C).

DISCUSSION

Using the model for epileptic spasms of unknown cause developed by the group of Velíšek, we examined whether the occurrence of spasms early in life affects synaptic function in the hippocampus later in life. We found that rats at postnatal week 6–11 (P42–P78) with a history of NMDA-triggered spasms at P12–15 showed enhanced LTP and a reduced frequency of excitatory synaptic transmission in CA1 pyramidal neurons.

In this model, a behavioral abnormality suggestive of impaired anxiety has been reported at P20–22, that is, 5–7 days after the spasms.[15] Hence, the present study provides an evaluation at the most developed stage, to our knowledge, of brain function in this model. Because it has been shown in many studies that the aberrant LTP results in various forms of memory deficit in experimental animals, it is an interesting future project to examine whether these models also show memory deficit in the behavioral tasks requiring hippocampal functions, as reported in a distinct model of NMDA-triggered epilepsy without prenatal steroid priming.[22]

Synaptic features in adult rats with a history of NMDA injections

Despite the significantly larger LTP magnitude in response to TBS and the significantly larger population of neurons with lower sEPSC frequency in the NMDA group than in the control group, the LTP magnitude in response to tetanus stimulation, the instantaneous response to TBS, the amplitude of baseline sEPSCs and sIPSCs, the PPR of fEPSP slope, the EPSC amplitude, and the NMDA/AMPA ratio in the CA1 in the NMDA group did not significantly differ compared to the control group. Altogether, it is less likely that the infantile NMDA treatment affected basic synaptic transmission properties at either presynaptic or postsynaptic levels including the membrane expression of NMDA receptors. It is more likely that the subcellular machinery and/or neuronal environment underlying LTP regulation is altered in these rats.

Such enhanced synaptic potentiation without changes in the NMDA/AMPA ratio is reminiscent of a similar LTP enhancement in mice lacking postsynaptic density-95 (PSD-95) protein.[23] Of interest, LTP in PSD-95-deficient

A Control   NMDA   NMDA/ACTH

B

C

D
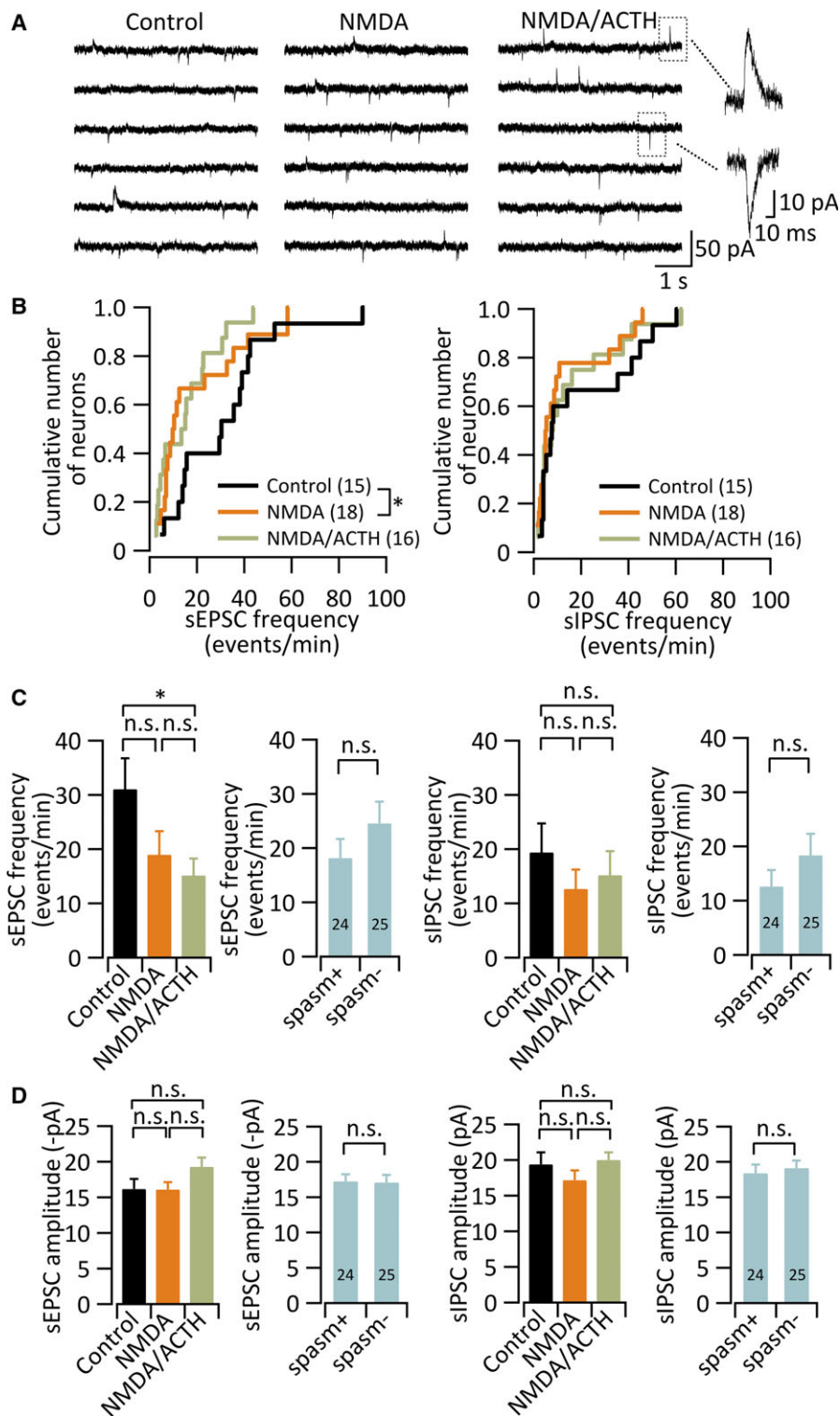
mice also depends largely on the frequency of stimulation,[23] suggesting that metaplastic regulation of the relationship between synaptic input and plasticity[24] is affected in this model. The authors of this report attributed these properties to modified intracellular processes downstream of glutamate receptor activation. Likewise, such a difference in

LTP-inducing effects between tetanus stimulation and TBS was also reported in an adult rat model of sustained status epilepticus induced by juvenile pilocarpine injection.[25] The authors of this study attributed this difference to the aberrantly augmented expression of NR2B subunits. Thus, it is possible that such changes in the subunit composition of

Figure 3.
Synaptic transmission in the adult hippocampus from rats with infantile NMDA injections and ACTH treatment. (**A**) Representative traces for continuous recording of the membrane currents of CA1 pyramidal neurons from control (left), NMDA (middle), and NMDA/ACTH (right) groups. The time-extended traces on the right show representative events for sIPSC (upward event) and sEPSC (downward event) waveforms. The equilibrium potential for Cl⁻ is −90 mV, and the holding potential was −60 mV. (**B**) The cumulative number of neurons (Y-axis) showing respective frequency (X-axis) of sEPSC (left) and sIPSCs (right). The sEPSCs and sIPSCs were detected from a continuous 5 min recording, and the frequency was calculated as total number of detected events divided by 5. Results of CA1 neurons from rats belonging to control (black curve), NMDA (orange curve), and NMDA/ACTH (olive green curve) groups. *p < 0.05, Kolmogorov-Smirnov test. Numbers in parentheses indicate the numbers of neurons. (**C**) Summary of sEPSC and sIPSC frequency in control (black bar), NMDA (orange bar), and NMDA/ACTH (olive green bar) groups. The graphs with pale blue bars (second and fourth from the left) show the comparison of sEPSC and sIPSC frequency for rats with or without spasms. Error bars represent SEM. *p < 0.05, one-way ANOVA with post hoc Tukey test. Two graphs on the left represent the results of sEPSC analyses and those on the right are those of sIPSC. The numbers in the bar show the number of neurons. (**D**) Summary of sEPSC and sIPSC amplitude in control (black bar), NMDA (orange bar), and NMDA/ACTH (olive green bar) groups. The graphs with pale blue bars (second and fourth from the left) show the comparison of sEPSC and sIPSC amplitude for rats with or without spasms. Error bars represent SEM. n.s., not significantly different (ANOVA). Two graphs on the left represent the results of sEPSC analyses and those on the right are those of sIPSC. The numbers in the bar show the number of neurons.
Epilepsia © ILAE

postsynaptic receptors might also underlie the enhanced LTP in the adult rats of our model.

In addition to exaggerated synaptic plasticity, the rats from the NMDA group without ACTH treatment also showed reduced sEPSC frequency. As there were no apparent differences in PPR, an indication of a lack of difference in release probability, possible mechanisms might include fewer synapses on the pyramidal neuron spine/dendrites in the NMDA group, which would await further morphologic examination. Because the recordings of EPSCs were made in slices in which the connections between CA3 and CA1 were cut, this smaller sEPSC frequency is not a result of the decreased spontaneous firing of CA3 pyramidal neurons. Further analyses are required to determine the underlying mechanism. Altogether, these lines of evidence suggest that NMDA-induced spasms early in life combined with prenatal maternal stress results in altered organization of plasticity-related molecules and modified synaptic transmission properties in adulthood. This is the first study to demonstrate aberrantly affected excitatory synaptic transmission in a model of epileptic spasms.

Mechanism for long-term influence

An important remaining question is how these remote and latent influences could occur. Because NMDA receptors are already functional in the hippocampus at this early stage,[26] a possibility is that intraperitoneal NMDA injection at P12–15 triggered Ca^{2+} entry through NMDA receptor channels in the hippocampus and directly affected the hippocampal network. However, this seems less likely because NMDA-triggered spasms do not significantly increase c-fos protein expression in the dorsal hippocampus, unlike many other structures in the limbic system, hypothalamus, and brainstem. These structures show marked c-fos expression at 30–120 min after the onset of spasms.[13] Rather, it would be more likely that the postnatal NMDA injection and subsequent spasms would alter the future development program

of the whole brain in a fragile state primed by prenatal steroid injection or stress.[27,28]

Of interest, the enhanced LTP was significantly related to repeated NMDA injections, not the occurrence of spasms (Fig. 2A2). It has been shown that, although early life seizures may not result in detectable hippocampal damage, long-term changes to hippocampal plasticity occur.[18,29] The present results are also in line with these examples of postmaturation alterations in hippocampal plasticity. This would suggest that the activation of NMDA receptors itself, probably outside of the hippocampus and in the areas showing increased c-fos expression after injection,[13] would be the key initial events leading to the aberrant synaptic organization observed later in life. Indeed, infantile NMDA injection alone leads to aberrant cognitive functions in adult rats.[22] Conversely, prenatal steroid injection[15] and behavioral stress[27] are potent primers for epileptic spasm-like behavior. The present study demonstrates clearly that such combined outcomes of prenatal priming and infantile NMDA injection lead to later aberrant synaptic development. In this study, ACTH treatment, which is effective in reducing spasms in human patients, did not significantly reduce the number of rats that experienced spasms of whatever duration but rather it significantly affected the distribution of the frequency of long (>5 s) spasm-like motion arrests appearing in each rat. This suggests that ACTH reduces severity of the influence of NMDA treatment at least in this model, which might be more related to the enhanced LTP after maturation. However, ACTH, at the administration protocol used in this study, was less effective in eliminating spasms than reported in human patients, suggesting that this model falls short of a complete phenocopy of the human situation. Thus, the interpretation is that a combination of prenatal stress and postnatal aberrant activation of the glutamate system would increase the risk of epileptic spasms with behavioral and neurologic effects in adulthood. Such an
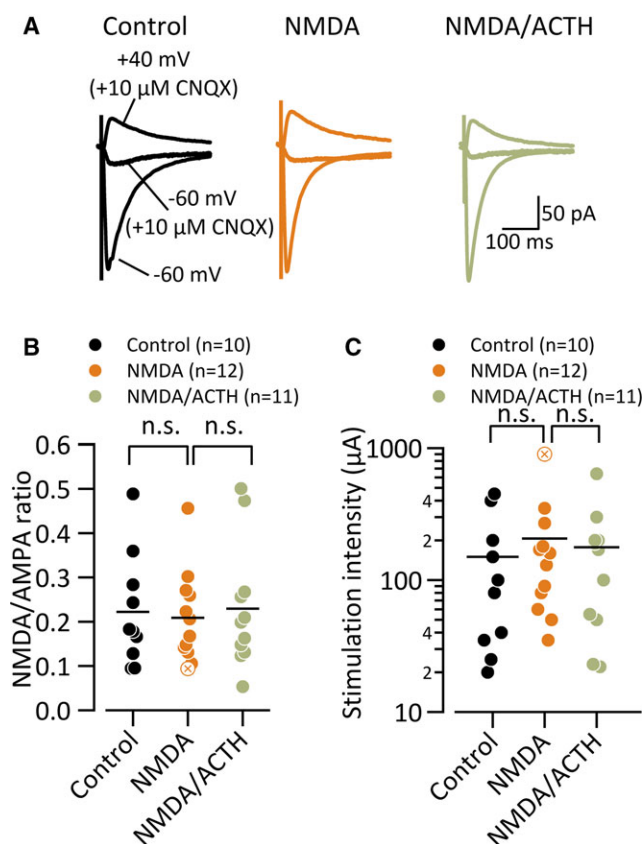
Figure 4.
NMDA/AMPA ratio of the excitatory transmission from the Schaffer collateral to pyramidal neurons in the CA1. (**A**) Representative traces of evoked EPSCs. Traces from bottom to top indicate AMPA receptor–mediated currents at a holding potential of −60 mV (average of 60 EPSCs), that in the presence of 10 μM CNQX (average of 3–4 traces) and NMDA receptor–mediated currents recorded at +40 mV in the presence of CNQX (average of 60 EPSCs). Representative neurons from rats belonging to control (black curves, left), NMDA (orange curves, middle), and NMDA/ACTH groups (olive green curves, right). (**B**) Summary of NMDA/AMPA ratios recorded in neurons from control (black circles), NMDA (orange circles), and NMDA/ACTH (olive green circles) groups. The circle with "X" indicates the values for slices from rats showing no detectable post-NMDA spasms at P15. (**C**) Summary of stimulus intensities required to evoke AMPA receptor–mediated postsynaptic currents with approximate amplitude of 200 pA. The circle with "X" indicates the values for slices from rats showing no detectable post-NMDA spasms at P15. The horizontal bars indicate the mean value for each group. n.s., not significantly different (ANOVA).
Epilepsia © ILAE

involvement of prenatal maternal stress was also suggested in an epidemiologic study by Shang et al.[30] It is thus imaginable that prenatal maternal stress would have a priming effect on the later expression of epileptic spasms and long lasting/remaining consequences that might affect emotional/cognitive functions due to aberrant synaptic organization in adulthood. It is important to develop other

types of epileptic spasms models in which spasms are spontaneously triggered, unlike the NMDA-dependent models used in this study, and compare with the findings described in this study. In addition, the present results also strengthen the need for more relevant models for West syndrome or epileptic spasms in terms of behavioral and electrophysiologic phenotypes together with treatment responses and late developmental consequences. It is worth noting that, despite the number of human genes known to cause epileptic spasms, none of their respective rodent models made at this moment phenocopies the symptoms.

Such a remote influence of epileptic states on brain activity early in life and behavior later in life has been documented in several models of other types of epilepsy, such as the complex febrile seizure model[31] and hypoxia-induced convulsion model.[18] Both of these studies report that acute treatment immediately after infantile convulsions with a KCC2 inhibitor (febrile seizures) or ionotropic glutamate receptor antagonist (hypoxia-induced convulsions) suppressed the aberrant neurologic symptoms during adulthood. These drug effects are reminiscent of the effect of ACTH in the NMDA/ACTH group in the present study in rectifying the aberrant LTP in adult rats. Therefore, an intriguing hypothesis is that ACTH compensates for the functional neuroendocrine aberrancy caused by prenatal stress and suppresses the cerebral events, thereby leading to NMDA receptor activation underlying the formation of aberrant synaptic organization during development. This hypothesis awaits future experimental support.

CONCLUSION

We showed alteration of synaptic transmission and plasticity in the hippocampus of adult rats with a history of NMDA-induced spasms in infancy. These findings will provide novel insights into a strategy for better cognitive outcome, beyond seizure control, in patients with epileptic spasms of unknown cause.

ACKNOWLEDGMENT

DISCLOSURE

REFERENCES

1. Dulac O. What is West syndrome? *Brain Dev* 2001;23:447–452.
2. Widjaja E, Go C, McCoy B, et al. Neurodevelopmental outcome of infantile spasms: a systematic review and meta-analysis. *Epilepsy Res* 2015;109:155–162.

3. Partikian A, Mitchell WG. Neurodevelopmental and epilepsy outcomes in a North American cohort of patients with infantile spasms. *J Child Neurol* 2010;25:423–428.

4. Trevathan E, Murphy CC, Yeargin-Allsopp M. The descriptive epidemiology of infantile spasms among atlanta children. *Epilepsia* 1999;40:748–751.

5. Kurokawa T, Goya N, Fukuyama Y, et al. West syndrome and Lennox-Gastaut syndrome: a survey of natural history. *Pediatrics* 1980;65:81–88.

6. Riikonen R. Long-term outcome of patients with West syndrome. *Brain Dev* 2001;23:683–687.

7. Lux A. Latest American and European updates on infantile spasms. *Curr Neurol Neurosci Rep* 2013;13:1–8.

8. Lee CL, Frost JD, Swann JW, et al. A new animal model of infantile spasms with unprovoked persistent seizures. *Epilepsia* 2008;49:298–307.

9. Cortez MA, Shen L, Wu Y, et al. Infantile spasms and Down syndrome: a new animal model. *Pediatr Res* 2009;65:499–503.

10. Marsh E, Fulp C, Gomez E, et al. Targeted loss of Arx results in a developmental epilepsy mouse model and recapitulates the human phenotype in heterozygous females. *Brain* 2009;132:1563–1576.

11. Price MG, Yoo JW, Burgess DL, et al. A triplet repeat expansion genetic mouse model of infantile spasms syndrome, Arx(GCG)10 + 7, with interneuronopathy, spasms in infancy, persistent seizures, and adult cognitive and behavioral impairment. *J Neurosci* 2009;29:8752–8763.

12. Scantlebury MH, Galanopoulou AS, Chudomelova L, et al. A model of symptomatic infantile spasms syndrome. *Neurobiol Dis* 2010;37:604–612.

13. Velíšek L, Jehle K, Asche S, et al. Model of infantile spasms induced by N-methyl-D-aspartic acid in prenatally impaired brain. *Ann Neurol* 2007;61:109–119.

14. Velíšek L, Chachua T, Yum M-S, et al. Model of cryptogenic infantile spasms after prenatal corticosteroid priming. *Epilepsia* 2010;51:145–149.

15. Chachua T, Yum M-S, Velíšková J, et al. Validation of the rat model of cryptogenic infantile spasms. *Epilepsia* 2011;52:1666–1677.

16. Go CY, Mackay MT, Weiss SK, et al. Evidence-based guideline update: medical treatment of infantile spasms: report of the Guideline Development Subcommittee of the American Academy of Neurology and the Practice Committee of the Child Neurology Society. *Neurology* 2012;78:1974–1980.

17. Notenboom RGE, Ramakers GMJ, Kamal A, et al. Long-lasting modulation of synaptic plasticity in rat hippocampus after early-life complex febrile seizures. *Eur J Neurosci* 2010;32:749–758.

18. Zhou C, Bell Lippman JJ, Sun H, et al. Hypoxia-induced neonatal seizures diminish silent synapses and long-term potentiation in hippocampal CA1 neurons. *J Neurosci* 2011;31:18211–18222.

19. Tsuji M, Takahashi Y, Watabe AM, et al. Hippocampal Synaptic Plasticity After Development in a Rat Model of Cryptogenic Infantile Spasms. Program No. 247.14. 2013 Neuroscience Meeting Planner: Society for Neuroscience, 2013. Online.

20. Watabe AM, O'Dell TJ. Age-related changes in theta frequency stimulation-induced long-term potentiation. *Neurobiol Aging* 2003;24:267–272.

21. Kawamura M, Gachet C, Inoue K, et al. Direct excitation of inhibitory interneurons by extracellular ATP mediated by P2Y1 receptors in the hippocampal slice. *J Neurosci* 2004;24:10835–10845.

22. Stafstrom CE, Sasaki-Adams DM. NMDA-induced seizures in developing rats cause long-term learning impairment and increased seizure susceptibility. *Epilepsy Res* 2003;53:129–137.

23. Migaud M, Charlesworth P, Dempster M, et al. Enhanced long-term potentiation and impaired learning in mice with mutant postsynaptic density-95 protein. *Nature* 1998;396:433–439.

24. Larson J, Munkácsy E. Theta-burst LTP. *Brain Res* 2015;1621:38–50.

25. Müller L, Tokay T, Porath K, et al. Enhanced NMDA receptor-dependent LTP in the epileptic CA1 area via upregulation of NR2B. *Neurobiol Dis* 2013;54:183–193.

26. Monyer H, Burnashev N, Laurie DJ, et al. Developmental and regional expression in the rat brain and functional properties of four NMDA receptors. *Neuron* 1994;12:529–540.

27. Yum M-S, Chachua T, Velíšková J, et al. Prenatal stress promotes development of spasms in infant rats. *Epilepsia* 2012;53:e46–e49.

28. Onishi M, Iinuma M, Tamura Y, et al. Learning deficits and suppression of the cell proliferation in the hippocampal dentate gyrus of offspring are attenuated by maternal chewing during prenatal stress. *Neurosci Lett* 2014;560:77–80.

29. Bender RA, Dubé C, Gonzalez-Vega R, et al. Mossy fiber plasticity and enhanced hippocampal excitability, without hippocampal cell loss or altered neurogenesis, in an animal model of prolonged febrile seizures. *Hippocampus* 2003;13:399–412.

30. Shang N-X, Zou L-P, Zhao J-B, et al. Association between prenatal stress and infantile spasms: a case-control study in China. *Pediatr Neurol* 2010;42:181–186.

31. Koyama R, Tao K, Sasaki T, et al. GABAergic excitation after febrile seizures induces ectopic granule cells and adult epilepsy. *Nat Med* 2012;18:1271–1278.